AIAA JOURNAL
Vol. 47, No. 7, July 2009

Acoustically Nonreflecting and Reflecting Boundary Conditions for Vorticity Injection in Compressible Solvers

Nicolas Guézennec* and Thierry Poinsot†
Institut de Mécanique des Fluides de Toulouse, 31400 Toulouse, France

DOI: 10.2514/1.41749

Injecting turbulence into computational domains is needed in many direct numerical simulations or large eddy simulations. This task may become difficult in compressible formulations in which acoustic waves must also be controlled on boundaries. In this paper, three characteristic boundary conditions are compared with inject isolated vortices or turbulence into the flow and control the acoustic behavior of the boundary at the same time. The first two methods are the usual characteristic boundary conditions (reflecting and nonreflecting Navier–Stokes characteristic boundary-condition techniques) used to introduce acoustic waves. The third one is a new boundary condition (vortical-flow characteristic boundary condition) constructed to introduce turbulence or vortices while being nonreflecting for acoustic waves. The three methods are tested in two academic cases: 1) injection of an isolated vortex and 2) injection of isotropic turbulence. These two tests are first performed in a quiet flow and then in a domain in which acoustic waves propagate toward the inlet and interact with vorticity injection. Results show that the reflecting Navier–Stokes characteristic boundary condition performs correctly to introduce vorticity waves (vortices or turbulence) and totally reflect acoustic waves. To introduce vorticity waves and let acoustic waves propagate without reflection, the vortical-flow characteristic boundary condition is required and the usual Navier–Stokes characteristic boundary-condition method cannot be used.

I. Introduction

DEVELOPING accurate boundary conditions is a major problem in the simulation of unsteady compressible flow problems such as astrophysics [1,2], aeroacoustics [3–6], or combustion instabilities [7,8]. Because acoustic waves propagate at high speed, interact with the flow, and are not dissipated by modern high-fidelity numerical methods, controlling their reflection or generation at boundaries has become a first-order issue in the development of most direct numerical simulation (DNS) and large eddy simulation (LES) codes in these fields.

It has been recognized for a long time that the best approach to handle such problems is to manipulate the amplitude of acoustic and entropy waves entering the computational domain [9–11]. Most methods are based on the same principle: they decompose the Navier—Stokes equations at the boundary to identify the contribution of waves going into the domain and waves leaving the domain. The latter are computed using one-sided derivatives and are not modified, whereas waves entering the domain are changed according to the boundary condition. The modification of the incoming-wave amplitudes is the main difficulty, and this is where the methods differ. Two main classes of methods can be identified:

1) For one-dimensional (1-D) methods, in some approaches, the amplitude of the incoming waves is fixed by assuming that the flow can be viewed locally as one-dimensional and inviscid {the local one-dimensional inviscid (LODI) relations [9,12]}. The influence of transverse (i.e., parallel to the boundary plane) and viscous terms is neglected. Such methods are used, for example, in DNS [13–16] or LES of reacting flows [17–19].

2) For multidimensional methods, the accuracy of 1-D methods is not sufficient for multiple problems, especially at outlets in which such methods generate noise when vortices leave the domain. In recent years, it has been shown that taking into account transverse terms in the specification of the incoming waves is an efficient solution to increase the accuracy of outlet boundary-condition treatments. Including transverse terms in the incoming-wave amplitudes can be done following various ideas but is not a straightforward task [20–22]. In most methods, a low-Mach-number expansion is used to guide the derivation of the incoming-wave amplitude [23,24].

Although most boundary-condition studies address the problem of outlets, the present work focuses on one specific issue that is not discussed often: the specification of inlet conditions in which turbulence must be injected while still maintaining nonreflecting conditions. This is a critical issue in DNS of jet noise [6,25] or in LES of combustors [8,26]: for example, when the flow entering the computational domain must contain a resolved turbulent component (generated to satisfy proper spectra and energy distribution), but acoustic waves propagating back to the inlet must not reflect on this boundary (Fig. 1). If acoustic waves generated in the combustor reflect on the inlet and interact again with the flow, the whole system can enter a state of self-sustained oscillations.

For such problems, there is a difficult tradeoff at the inlet in that the boundary condition must impose the mean flow profile, inject turbulent perturbations, and still be nonreflecting for acoustic waves[‡]; for example, imposing the velocity $u(x, y, z, t)$ in an inlet plane to be exactly equal at each instant to a target value $u^t(x, y, z, t)$ (corresponding to the instantaneous turbulent signal to be injected) will obviously ensure the proper inlet turbulent flow but will also totally reflect acoustic waves, because the inlet velocity will not depend on outgoing waves. On the other hand, any attempt to make the inlet section perfectly nonreflecting might lead to an inlet velocity drifting away from the target field.

Finding a proper compromise to define inlet boundary conditions in which turbulence is injected and acoustic reflections are controlled is the objective of the present work. To reach this goal, a new nonreflecting boundary condition adapted to the introduction of vortical flows and called the vortical-flow characteristic boundary

Received 21 October 2008; revision received 2 February 2009; accepted for publication 7 April 2009.

*Ph.D. Student, Allée Camille Soula.

†Research Director, Allée Camille Soula; Institut National Polytechnique de Toulouse, Centre National de la Recherche Scientifique. Associate Fellow AIAA.

‡This difficulty is a specificity of fully compressible codes; in incompressible or low-Mach-number formulations, the problem does not appear because acoustic waves are not computed. This is an obvious disadvantage of compressible codes and a real problem in flows that definitely require compressible solvers.

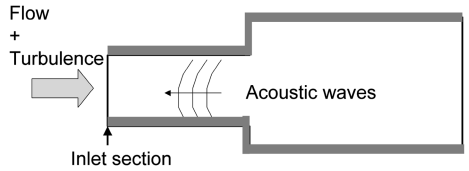

Fig. 1 Combustor nonreflecting inlet: turbulence must be injected, but acoustic waves must be able to leave with limited reflections.

condition (VFCBC) will be constructed on the basis of recent results obtained by Prosser [23,24], which allow to separate wave contributions due to acoustic and vorticity waves. VFCBC differs from the original Navier–Stokes characteristic boundary-condition (NSCBC) formulation [9], showing that the introduction of vortical flows on a nonreflecting inlet cannot be done with methods adapted to the introduction of acoustic waves.

The methods proposed subsequently will be compared in two relevant test cases: introduction of a single vortex in a quiet domain and introduction of two-dimensional synthetic turbulence in a quiet domain.

To illustrate the acoustic behavior of each formulation, the same test cases will then be repeated in cases in which acoustic waves propagate back toward the inlet. This study focuses on inlets, and for these cases, preliminary studies have shown that multidimensional methods did not bring significant advantages. Therefore, all subsequent methods are based on 1-D methods.

II. Nonreflecting Inlet Boundary Condition for Subsonic Vortical Flows

A. Local One-Dimensional Inviscid Relations at an Inlet

Consider a subsonic inlet in which turbulence must be injected and assume that the boundary plane is the x_2–x_3 plane. The velocity components to impose at this inlet will be written as U^t, V^t, and W^t. These target values can be obtained by running a separate 3-D solver and reading it plane by plane using Taylor's assumption [27,28] or by generating a synthetic turbulent signal based on digital filters [29,30] or on inverse Fourier techniques [31,32]. The NSCBC procedure [33] is one of the usual methods used to evaluate the amplitude of the incoming waves L_i. This approach is based on the assumption that the flow is locally one-dimensional and inviscid. LODI equations link the wave amplitudes L_i and the temporal evolution of primitive Navier–Stokes variables (ρ, u_1, u_2, u_3, and p). Their expressions are obtained through characteristic analysis of the one-dimensional Euler equations [7,9,10]:

$$\frac{\partial \rho}{\partial t} + \frac{1}{c^2}\left(-L_2 + \frac{1}{2}(L_5 + L_1)\right) = 0 \tag{1}$$

$$\frac{\partial u_1}{\partial t} + \frac{1}{2\rho c}(L_5 - L_1) = 0 \tag{2}$$

$$\frac{\partial u_2}{\partial t} + L_3 = 0 \tag{3}$$

$$\frac{\partial u_3}{\partial t} + L_4 = 0 \tag{4}$$

$$\frac{\partial p}{\partial t} + \frac{1}{2}(L_5 + L_1) = 0 \tag{5}$$

The wave amplitudes L_1, L_2, L_3, L_4, and L_5 correspond, respectively, to the left-traveling acoustic wave (speed $u_1 - c$), the entropy wave (speed u_1), the two vorticity waves (speed u_1), and the right-traveling acoustic wave (speed $u_1 + c$). LODI equations can be cast for all variables. For example, the LODI equation for temperature T is

$$\frac{\partial T}{\partial t} + \frac{T}{\gamma p}\left(-L_2 + \frac{1}{2}(\gamma - 1)(L_5 + L_1)\right) = 0 \tag{6}$$

For a subsonic inlet, four incoming waves L_2, L_3, L_4, and L_5 must be imposed, which is equivalent to imposing the three velocity components u_i and the temperature T. Independent of the nature of the transverse fluctuations V^t and W^t to impose at the inlet, the natural solution for L_3 and L_4 is

$$L_3 = -\frac{\partial V^t}{\partial t} \quad \text{and} \quad L_4 = -\frac{\partial W^t}{\partial t} \tag{7}$$

These conditions are nonreflecting because they do not depend on the outgoing wave L_1. The question is now how to construct L_2 and L_5 to obtain a nonreflecting boundary condition for normal velocity and temperature.

B. Determination of L_2 and L_5 to Inject Acoustic Waves

First, assume that the normal target velocity $U^t(t)$ (the value which u_1 must take at the inlet) is due to an acoustic wave entering the domain. Using the LODI relations (2) and (6), a natural solution is to write

$$L_5 = L_1 - 2\rho c\frac{\partial U^t}{\partial t} \quad \text{and} \quad L_2 = (\gamma - 1)\left(L_1 - \rho c\frac{\partial U^t}{\partial t}\right) \tag{8}$$

However, this boundary condition is reflecting [34]. To inject an acoustic wave and avoid reflections, the incoming waves L_5 and L_2 must not depend on the outgoing wave L_1, and the proper expression for L_5 is

$$L_5 = -2\rho c\frac{\partial U^t}{\partial t} \quad \text{and} \quad L_2 = -(\gamma - 1)\rho c\frac{\partial U^t}{\partial t} \tag{9}$$

where U^t is still the target value. Note that U^t is now the value that u_1 should follow in the absence of any reflected wave. If a wave is reflected toward the inlet, the inlet value u_1 will differ from U^t and the inlet will remain nonreflecting.

C. Determination of L_2 and L_5 to Inject Vortical Flows (VFCBC)

In the case of turbulence injection, the target velocity U^t is replaced by a signal corresponding to a vortical flow (vortices, homogeneous isotropic turbulence, etc.). A first solution is to use the boundary condition (8):

$$L_5 = L_1 - 2\rho c\frac{\partial U^t}{\partial t}x \tag{10}$$

Condition (10) has been used successfully for academic DNS or LES with high-order schemes and simple geometries (Guichard et al. [27]). But for configurations with strong acoustic phenomena such as combustion in a gas turbine, a nonreflecting condition is often required. Condition (9) is an obvious possibility, which will be tested subsequently; results will show that values for velocity and vorticity obtained with condition (9) do not match the expected values. Therefore, a better condition was sought.

First, the reason that condition (9) may not be adapted for turbulence injection must be understood: both turbulence and acoustic waves produce velocity and pressure perturbations, but interpreting turbulence effects (which are essentially incompressible) such as acoustic waves [as done in both Eqs. (9) and (10)] is the source of the problem. This question has been analyzed recently in multiple papers, even though no unique solution was identified [20,23,35]. For example, by distinguishing acoustic from inertial contributions and performing an expansion in Mach number on the Euler equations, Prosser [23] showed that the interaction between inertial structures (turbulence) and acoustic appears for the zeroth-order velocity terms and for the second-order pressure terms.

This result allows a simple derivation of a new boundary condition (VFCBC) to inject turbulence without acoustic reflection or

interaction. If we only consider the zeroth-order terms and assume that vortical-flow injection creates no acoustic pressure, the Mach number expansion of Prosser [23] for the equations of u_1 and p becomes

$$\frac{\partial u_1}{\partial t} + u_1 \frac{\partial u_1}{\partial x_1} = 0 \quad \text{and} \quad \frac{\partial p}{\partial t} = 0 \tag{11}$$

Equation (11) provides an evaluation of the wave amplitudes needed in NSCBC for an injection of turbulence (at low speed and low Mach number). These waves are

$$\begin{aligned} L_1 &= -\left(\frac{\partial p}{\partial t} - \rho c \frac{\partial u_1}{\partial t}\right) = \rho c \frac{\partial U^t}{\partial t} \quad \text{and} \\ L_5 &= -\left(\frac{\partial p}{\partial t} + \rho c \frac{\partial u_1}{\partial t}\right) = -\rho c \frac{\partial U^t}{\partial t} \end{aligned} \tag{12}$$

and so the proper expressions for the incoming waves L_5 and L_2 are

$$L_5 = -\rho c \frac{\partial U^t}{\partial t} \quad \text{and} \quad L_2 = 0 \tag{13}$$

Equation (13) shows that L_5 differs by a factor of 2 from Eq. (9), which was the nonreflecting condition for acoustic wave injection. This is the first surprise of this derivation. A second one is that the amplitude of the outgoing wave L_1 should be equal to $-L_5$ according to Eq. (12). In a subsonic flow, the amplitude L_1 depends on the flow within the domain and cannot be fixed or assumed to take a predetermined value like $-L_5$. Prosser [23] explained this paradox by recalling that the amplitudes of L_1 and L_5 chosen at the boundary must be viewed as the values of L_1 and L_5 for the *frozen turbulent flow* that is injected in the absence of any acoustic wave reflected from the domain to the inlet section. Another way to interpret the expression of L_5 [Eq. (13)] is to view it as the sum of two contributions: 1) the frozen injected turbulent flow and 2) the acoustic contribution:

$$L_5 = -\rho c \frac{\partial U^t}{\partial t} + 0 \tag{14}$$

where the first right-hand-side term corresponds to the frozen injected turbulent flow and the second one corresponds to the acoustic contribution. This shows that Eq. (14) is actually a nonreflecting condition for acoustics, even though the total amplitude of the injected wave is nonzero. Similarly, the outgoing-wave amplitude L_1 can be written

$$L_1 = \rho c \frac{\partial U^t}{\partial t} + L_1^a \tag{15}$$

where L_1^a is the amplitude of the outgoing acoustic waves, which cannot be fixed because it comes from the inside of the domain. As announced, this implies that the boundary conditions must differ when injecting acoustic waves (which are compressible signals in which p and u_1 signals always are of the same order: $p \simeq \rho c u_1$) or when injecting turbulence (for which pressure perturbations scale like the Mach number and vanish, in comparison with $\rho c u_1$, when the Mach number is small).

To summarize, Table 1 shows that three types of boundary condition can be used to inject perturbation at an inlet:

1) Method 1 is the reflecting NSCBC formulation.
2) Method 2 is the nonreflecting NSCBC formulation.
3) Method 3 is the nonreflecting VFCBC formulation.

The next sections compare these three methods in various reference cases.

III. Simple Test Case: Injection of a 2-D Inviscid Vortex

To illustrate the demonstration of the precedent section and to compare the methods of Table 1, the configuration of a 2-D inviscid vortex entering a box is first tested. This is the simplest test case of vortical-flow injection and its analytical solution can be easily explicited for comparison with simulations.

A. Single Vortex Problem

The velocity field of a vortex convected by a steady flow ($\underline{u} = [\bar{U}_1, 0]$) is defined using the stream function:

$$\begin{pmatrix} u_1 \\ u_2 \end{pmatrix} = \begin{pmatrix} \frac{\partial \psi}{\partial X_2} \\ -\frac{\partial \psi}{\partial X_1} \end{pmatrix} \quad \text{and} \quad \psi = C \exp\left(-\frac{r^2}{2r_v^2}\right) \tag{16}$$

where $r = \sqrt{X_1^2 + X_2^2}$, C is the vortex strength, and r_v is a characteristic radius. From Eq. (16), the radial and tangential velocity fields are given by

$$u_r = 0 \quad \text{and} \quad u_\theta = \frac{Cr}{r_v^2} \exp\left(\frac{-r^2}{2r_v^2}\right) \tag{17}$$

and the distribution of vorticity is

$$\omega(r) = C\left(\frac{2r_v^2 - r^2}{r_v^4}\right) \exp\left(-\frac{r^2}{r_v^2}\right) \tag{18}$$

The momentum equation shows that such a vortex must have a radial pressure distribution that satisfies

$$\frac{\partial p}{\partial r} = \frac{\rho u_\theta^2}{r} \tag{19}$$

Assuming that the flow has a constant speed of sound c, the expression for pressure can be derived as [23,36]

$$p(r) = p_0 \exp\left(-\frac{\gamma}{2}\left(\frac{C}{r_v c}\right)^2 \exp\left(-\frac{r^2}{r_v^2}\right)\right) \tag{20}$$

These results are expressed in a frame of reference (X_1, X_2) attached to the vortex. In the absence of viscous dissipation, this analytical solution can be used for validation. For this test case, the computational domain is a 2-D square box $L \times L$. Periodic boundary conditions are defined on the edges $x_2 = \pm L/2$. To avoid any discrepancies due to the interaction between the vortex and the periodic edges, the stream function is periodized:

$$\psi = C \sum_{k=-p}^{p} \exp\left(-\frac{r^{k2}}{2r_v^2}\right) \tag{21}$$

where $r^k = \sqrt{X_1^2 + (X_2 + kL)^2}$. In the limit $p \to \infty$, the stream function ψ becomes periodic.

B. Test-Case Conditions

The computational domain is a 2-D square box of dimension $L = 1$ mm and of resolution 128^2. Fluid is air at ambient

Table 1 Incoming-wave amplitudes L_2 and L_5 for subsonic flows for steady state and vortical-flow injection

Method	Steady state	Vortical-flow injection
1: NSCBC reflecting	$L_5 = L_1$ $L_2 = 0$	$L_5 = L_1 - 2\rho c \frac{\partial U^t}{\partial t}$ $L_2 = (\gamma - 1)(L_1 - \rho c \frac{\partial U^t}{\partial t})$
2: NSCBC nonreflecting	$L_5 = 0$ $L_2 = 0$	$L_5 = -2\rho c \frac{\partial U^t}{\partial t}$ $L_2 = -(\gamma - 1)\rho c \frac{\partial U^t}{\partial t}$
3: VFCBC	$L_5 = 0$ $L_2 = 0$	$L_5 = -\rho c \frac{\partial U^t}{\partial t}$ $L_2 = 0$

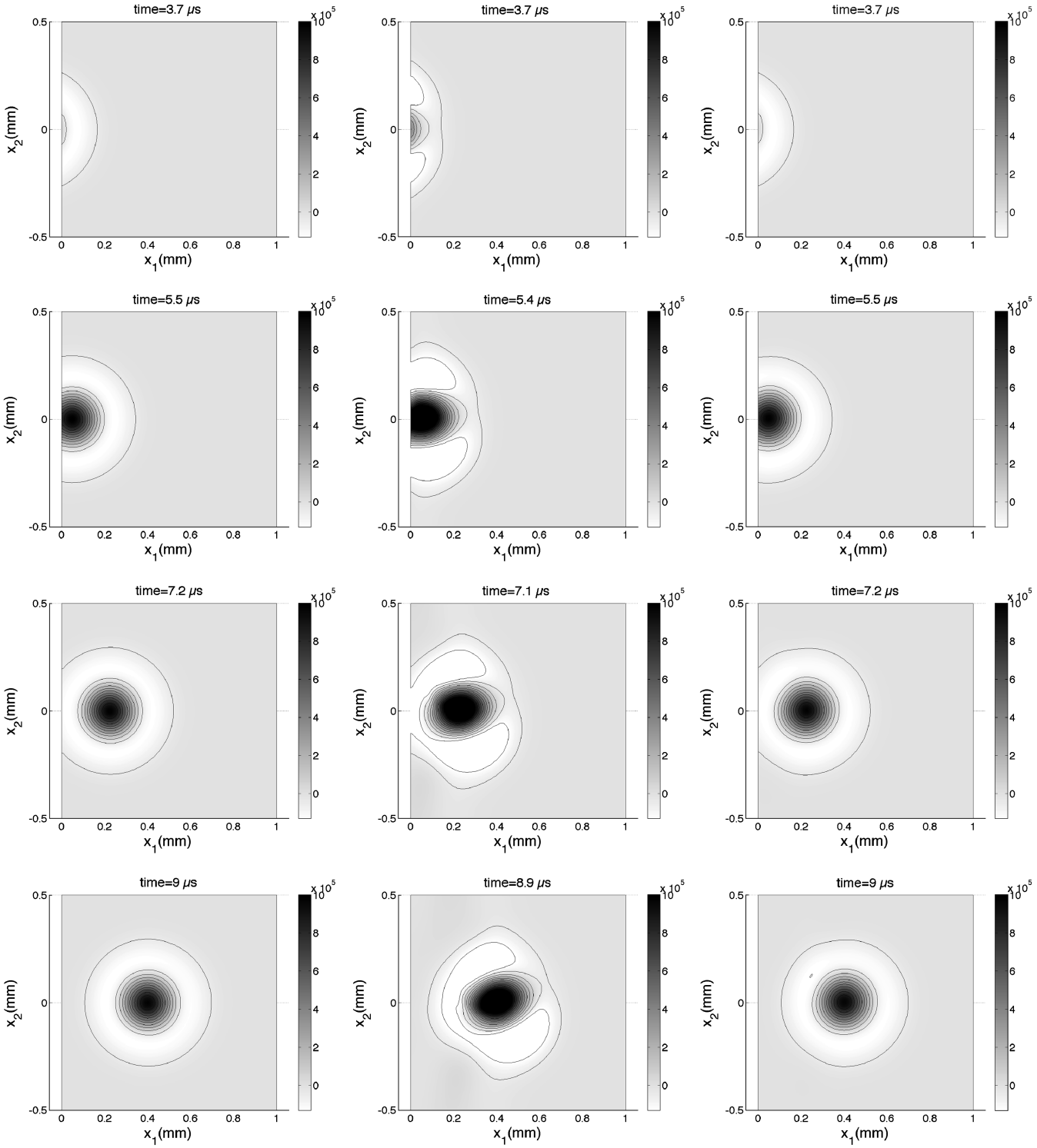

a) NSCBC (Reflecting) **b) NSCBC (Non-reflecting)** **c) VFCBC**

Fig. 2 Vorticity contours ω (s^{-1}).

pressure $p_0 = 1013$ hPa, and temperature $T_0 = 300$ K. C is set to 5×10^{-3} m^2/s, leading to a maximum vortex induced velocity of 30 m/s; r_v is 0.1 mm; and the mean velocity $\bar{U}_1$ is 100 m/s. For this test case, setting $p = 5$ in Eq. (21) is enough to ensure a good periodicity of the flow at $x_2 = \pm L/2$.

A two-step Galerkin finite element scheme is used to compute convective terms in Navier–Stokes equations. This scheme is called two-step Taylor–Galerkin version C [37] and is combined with a two-step Runge–Kutta method for time integration. It is third order in space and time and has a low dissipative error.

C. Results

Figures 2 and 3 show a series of vorticity and pressure contour plots comparing the new boundary condition VFCBC (method 3) with the two NSCBC approaches (methods 1 and 2). Figure 4 presents the evolution of the vorticity and the pressure drop with time at the inlet of the domain. The NSCBC reflecting boundary-condition solution matches the analytical solution perfectly. In contrary, strong deformations of the contour plot are observed in the NSCBC nonreflecting case, showing that this boundary condition is not adapted to inject a vortical wave. The VFCBC approach significantly

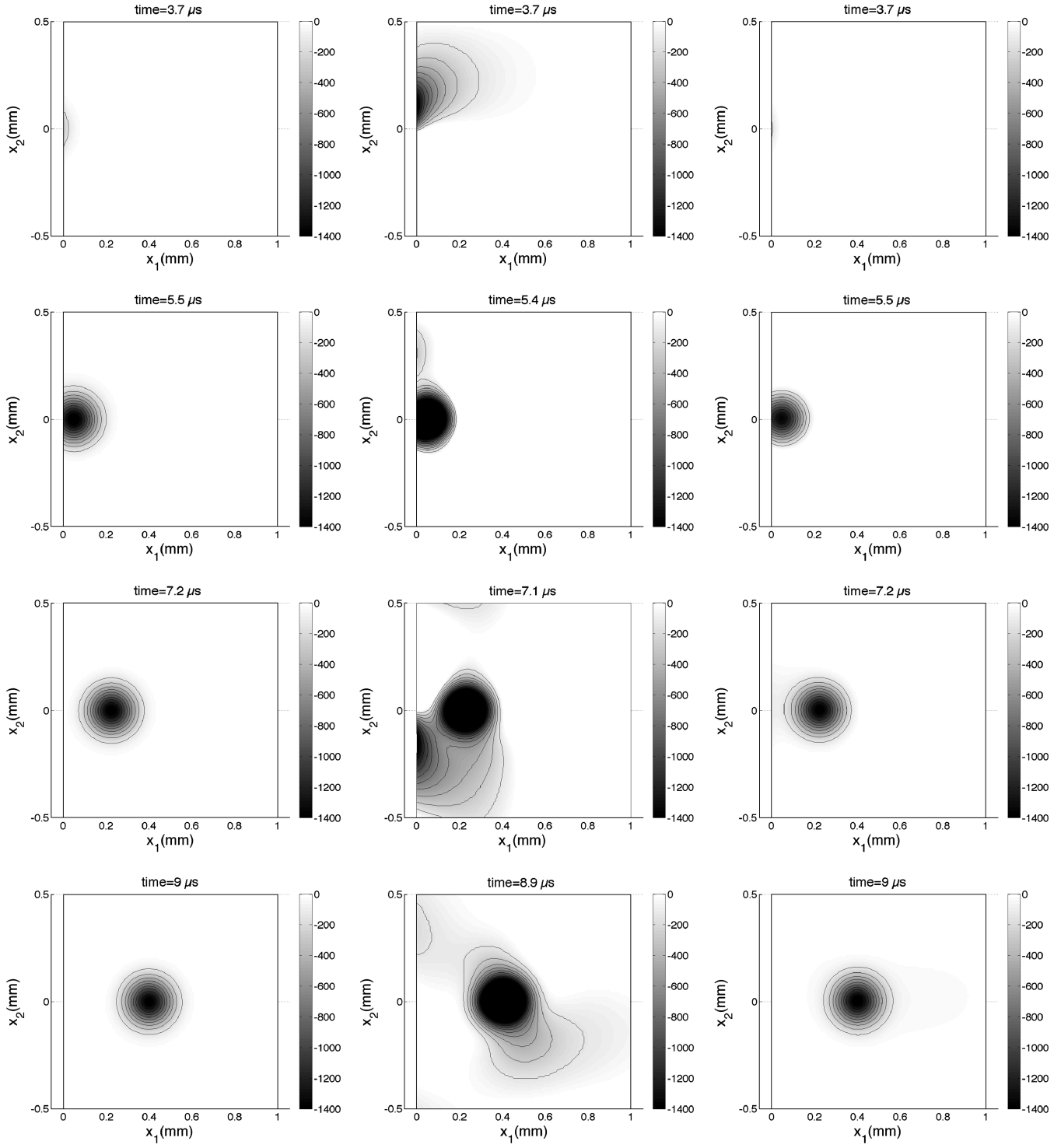

a) NSCBC (Reflecting) **b) NSCBC (Non-reflecting)** **c) VFCBC**

Fig. 3 Pressure contours $P - P_0$ in pascals.

reduces the observed errors. Pressure and vorticity contours remain symmetrical as the vortex traverses the boundary. In Fig. 4a, the vorticity curve matches the analytical solution perfectly. Only an underestimation of the pressure drop by 10 to 15% can be observed in the center of the vortex.

IV. Spatially Decaying Turbulence in a 2-D Periodic Box

The test case of the spatially decaying turbulence has been retained to evaluate the ability of the three methods of Table 1 to impose turbulent inlet boundary conditions, respecting correct statistics. In practice, at every time step, an homogeneous isotropic turbulent flow is injected at the inlet of a 2-D square box. This section first explains the methodology used to compute the synthetic turbulent signal entering the domain and then compares instantaneous turbulent fields and statistics for the three methods: reflecting NSCBC (method 1), nonreflecting NSCBC (method 2), and VFCBC (method 3).

A. Methodology for the Turbulence Injection

To generate the artificial turbulent flow entering the periodic domain, an extension of the Kraichnan method [38,39] was derived.

The flow is directly written in physical space, but instead of decomposing the velocity field in Fourier modes, a formulation based on the stream function is used to make it periodic. The turbulent flow is described as the sum of N periodic Gaussian vortices randomly placed in a 2-D box of dimension $L_1 \times L_2$. Periodicity is ensured by summing the stream function over $2p+1$ boxes (p boxes over and p boxes below the computational box). Therefore, the stream function is written

$$\Psi(x_1,x_2)=\sum_{n=0}^{N}\psi_n(x_1,x_2) \quad \text{with}$$
$$\psi_n(x_1,x_2)=C_n\sum_{k=-p}^{p}\exp\left(-\frac{r_n^{k2}}{2r_{vn}^2}\right) \tag{22}$$

where

$$r_n^k=\sqrt{(x_1-x_{1n})^2+(x_2-x_{2n}+kL_2)^2}$$

To ensure homogeneity, the position of each vortex (x_{1n}, x_{2n}) is chosen from a 2-D uniform distribution. The vortices' strengths C_n and the inverse values of the characteristic radii r_{vn}^{-1} are generated using isotropic Gaussian distributions of standard deviations C_0 and r_{v0}^{-1}. The parameters C_0 and r_{v0} must be set so that the desired length scale and turbulent intensity would be obtained in the limit $N \to \infty$. Using Eq. (22), the velocity field $\underline{u}$ and the vorticity field ω can be easily calculated, as well their statistics. Assuming that $N \to \infty$ and $r_{v0} \ll L_1$ and L_2, it can be shown that the expressions of the turbulent kinetic energy K_0 and the dissipation rate ϵ_0 are

$$K_0=\frac{(\bar{u}_1'^2+\bar{u}_2'^2)}{2}=\frac{\pi N C_0^2}{2L_1L_2} \quad \text{and} \quad \epsilon_0=2\nu_0\bar{\omega}'^2=4\nu_0\frac{K_0}{r_{v0}^2} \tag{23}$$

Figure 5a presents a vorticity field generated with this technique in a 2-D square box of dimension $L = 1$ mm. The parameter for this example are $N = 10000$, $p = 5$, $r_{v0} = 5.10^{-5}$ m, and $K_0 = 100\ \mathrm{m^2/s^2}$. The grid resolution is 128^2. As expected, the periodicity on the box edges $x_2 = \pm L/2$ is respected. Figure 5b shows the statistic distribution of u_1' and u_2'. For this number of vortices, the flow has a good degree of isotropy.

This frozen turbulence is injected in the domain at the mean velocity $\bar{U}_1$ using Taylor's assumption. Note that this method does not require any inverse Fourier transform or digital filter algorithm, which makes it very simple to implement in a solver to generate 2-D turbulent boundary conditions. Moreover, it does not require the construction of a two-dimensional turbulent field: only the flow on the inlet patch is computed at every time step. This is another advantage in terms of memory usage.

B. Results

The domain is a 2-D square box of dimension $L = 1$ mm with a resolution of 128^2. The spanwise direction is periodic. A reflecting boundary condition is imposed on the outlet [9]. Numerical methods are the same as in Sec. III.B. The configuration can be viewed as a simple model for the inlet pipe of a combustor. Fluid is air at ambient

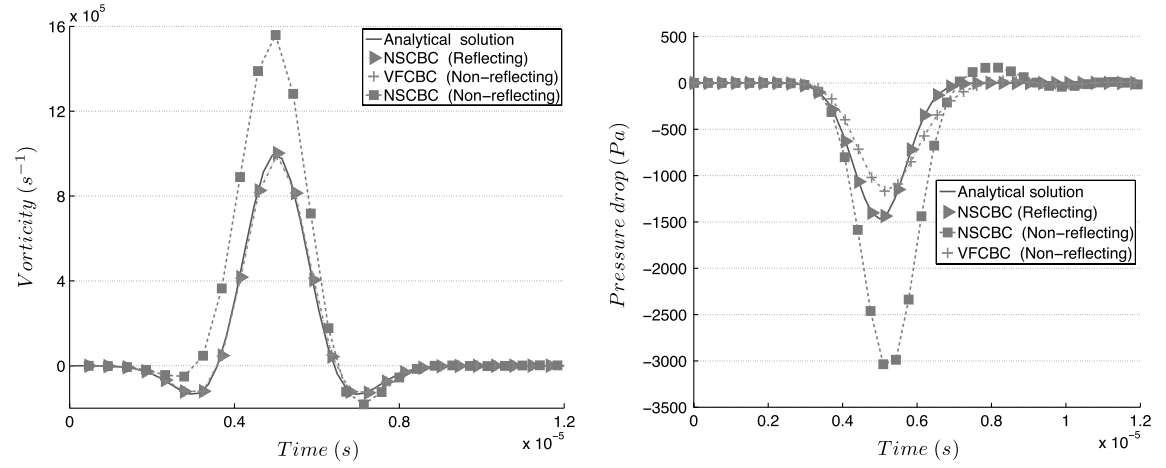

a) b)

Fig. 4 Evolution of vorticity and pressure versus time at the inlet of the computational domain ($x_1 = 0$ and $x_2 = 0$).

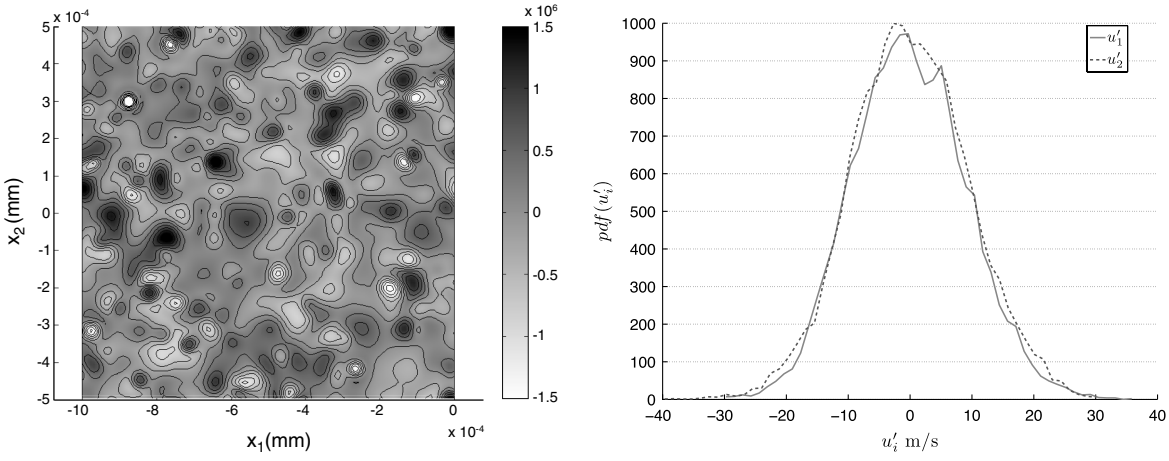

a) Vorticity field (s^{-1}) **b) Probability density functions of the velocity**

Fig. 5 Example of a 2-D periodic turbulent field generated with the potential method in a 1 × 1 mm box.

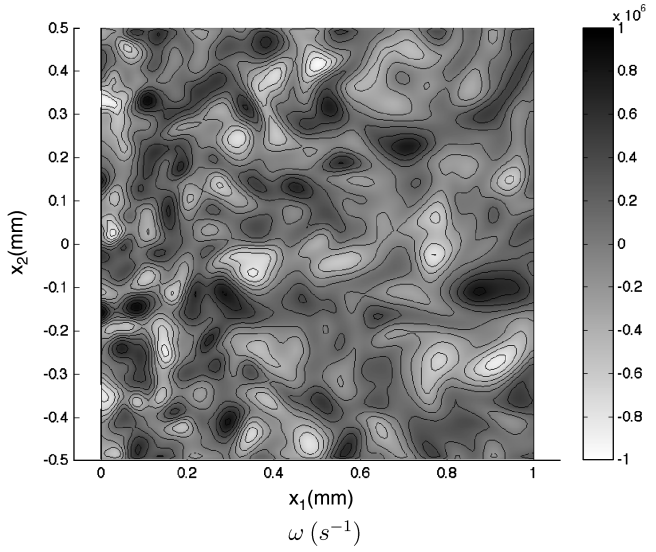

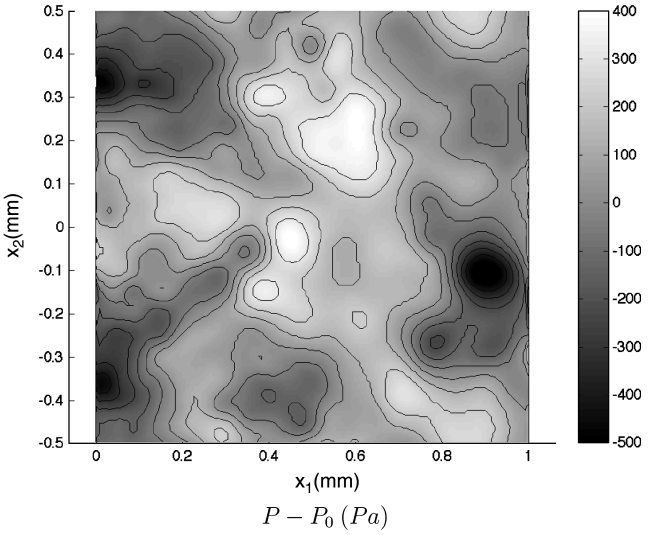

a) NSCBC (Reflecting)

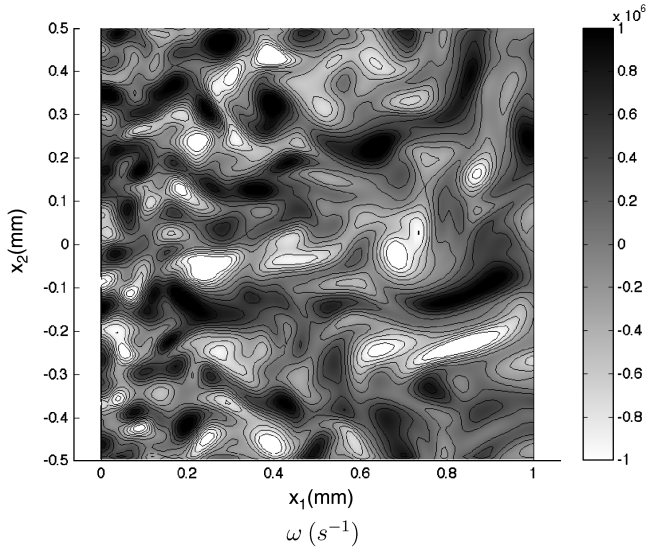

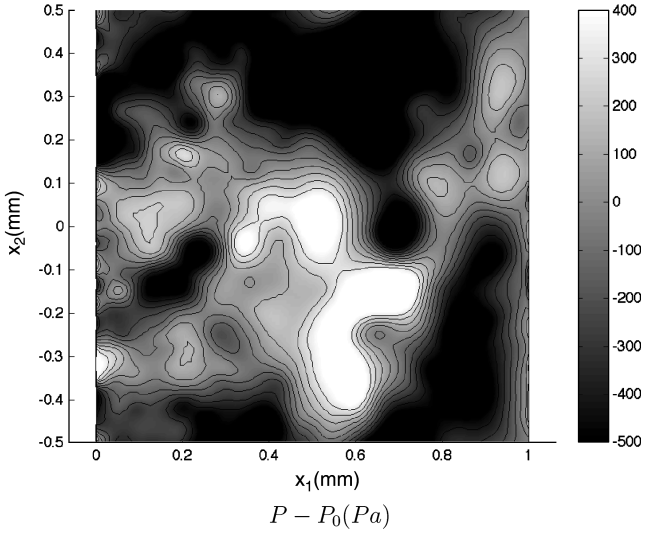

b) NSCBC (Non-reflecting)

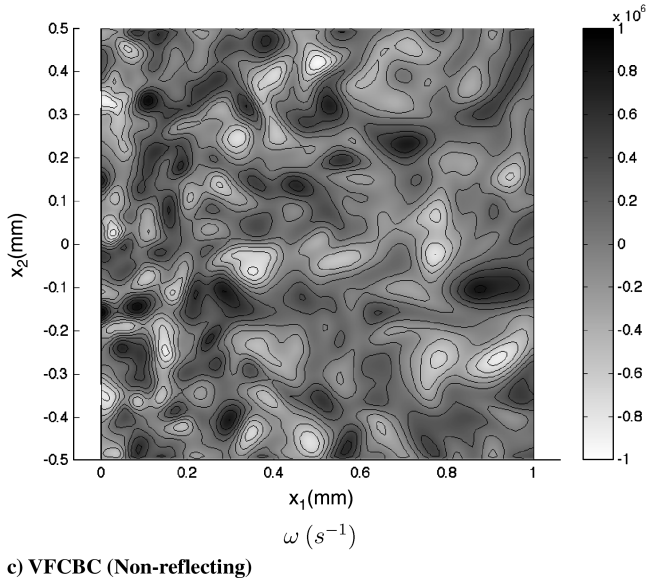

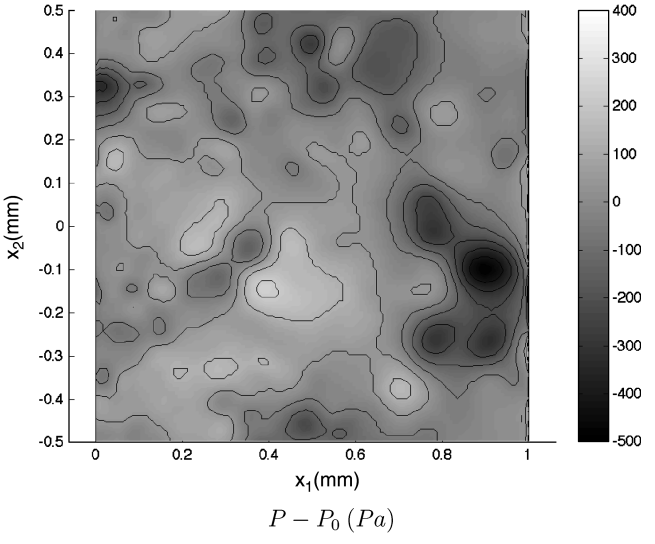

c) VFCBC (Non-reflecting)

Fig. 6 Vorticity and pressure fields $t = 40$ μs.

pressure $p_0 = 1013$ hPa and temperature $T_0 = 300$ K. The mean velocity is $\bar{U}_1 = 100$ m/s. The simulation duration corresponds to a physical time $T = 5(\bar{U}_1/L)$. Therefore, the dimensions of the box containing the injected turbulent flow are $L_1 = 5L$ and $L_2 = L$. The other parameters are $N = 50,000$, $p = 5$, $r_{v0} = 5.10^{-5}$ m, and $K_0 = 100$ m^2/s^2.

Figure 6 presents instantaneous vorticity and pressure fields for the three methods. Vorticity fields are nearly identical for the VFCBC and the reflecting NSCBC simulation, whereas the nonreflecting NSCBC simulation generates higher levels of vorticity. Conclusions concerning pressure are similar. The reflecting NSCBC (method 1) and VFCBC (method 3) simulations generate very low pressure fluctuations (less than 500 Pa), whereas the nonreflecting NSCBC simulation (method 2) leads to longer pressure oscillation levels.

The averaged properties of the turbulent field are displayed in Fig. 7. First, for the reflecting NSCBC and the VFCBC methods, the injection levels of the kinetic energy K and dissipation rate ϵ correspond to the theoretical values K_0 and ϵ_0 given by Eq. (23). Turbulence decays along the streamwise direction for the two methods. On the other hand, the nonreflecting NSCBC method presents important discrepancies. The levels of ϵ and K at $x_1 = 0$ are more than twice the theorical values K_0 and ϵ_0; just downstream of the inlet ($x = 0.1$ mm), the curve of K presents a nonphysical production of kinetic energy. It is also of interest to analyze pressure fluctuations for the three methods. The order of pressure fluctuations in a turbulent flow is typically equal to $\rho u_1'^2$. It is very low in comparison with an acoustic wave, in which pressure perturbations scale like $\rho c u_1'$. Therefore, for a compressible solver, it is crucial that the formulation of the turbulent inlet boundary condition generates as little noise as possible. Figure 7c presents the streamwise evolution of the pressure fluctuations normalized with the turbulent dynamic pressure $\rho_0 K_0$ for the three methods. Results observed on the instantaneous pressure fields (Fig. 6) are confirmed: the nonreflecting NSCBC simulations (method 2) generates abnormal levels of pressure fluctuations in the whole domain. The VFCBC (method 3) and the reflecting NSCBC methods (method 1) significantly improve these results.

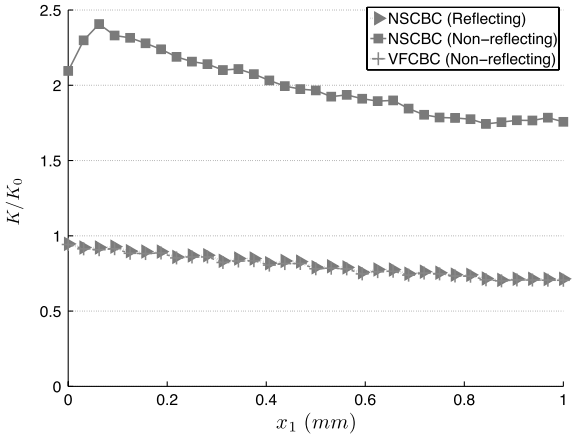

a) Normalized turbulent kinetic energy K/K_0

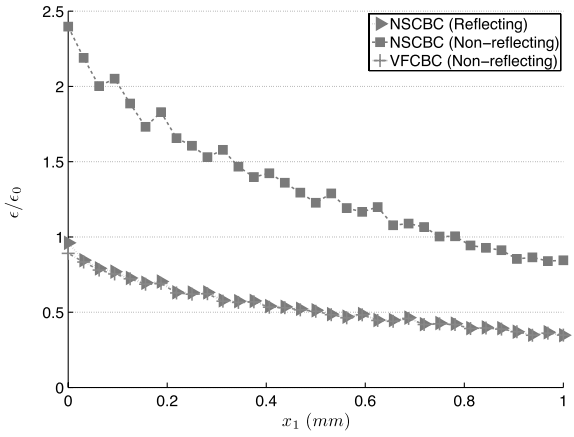

b) Normalized dissipation rate ϵ/ϵ_0

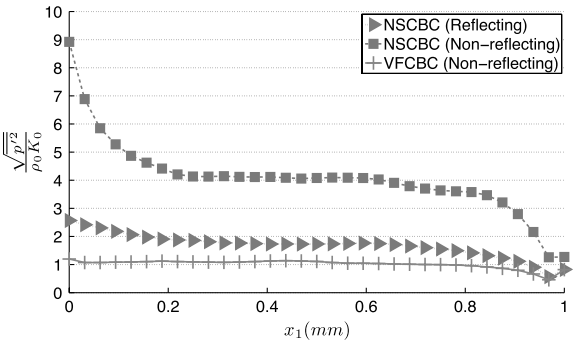

c) Normalized pressure fluctuations

Fig. 7 Streamwise evolution of the mean properties of the turbulence. Comparison of the three boundary conditions.

V. Acoustic Properties of Inlet Boundary Conditions

The two previous sections demonstrate similar abilities for the VFCBC (method 3) and the reflecting NSCBC (method 1) formulations to inject vortical flows with correct dynamic statistics $(K, \epsilon, \ldots)$. The two methods, however, have different acoustic behaviors. The reflecting NSCBC inlet totally reflects acoustic waves, whereas a VFCBC formulation is written so that acoustic waves can leave the computational domain. This section illustrates the latter key point. In the two previous sections (vortex and turbulence injection), boundary conditions were tested by injecting vortical flows into a quiet domain. In the present section, the same tests are repeated but the domain is not quiet anymore: acoustic perturbations are added to investigate their effects on the inlet boundary condition.

A. Injection of a 2-D Inviscid Vortex with an Acoustic Disturbance

For this test, an acoustic wave propagating toward the inlet interacts with a vortex entering the computational domain. The vortex characteristics and the computational domain are similar to the first section. The initial acoustic perturbation has a Gaussian shape and is centered in the middle of the studied domain. It corresponds to a left-traveling wave in which fluctuations of pressure and speed at time $t = 0$ are such that

$$p_{\mathrm{ac}} = -\rho_0 c_0 u_{\mathrm{ac}} \tag{24}$$

where $p_{\mathrm{ac}} = p_{\mathrm{ac0}} f(x)$ and $f(x)$ is a Gaussian perturbation,

$$f(x) = \exp\left(-\frac{(x_1 - x_{10})^2}{\sigma^2}\right)$$

so that

$$u_{\mathrm{ac}} = -\frac{p_{\mathrm{ac0}}}{\rho_0 c_0} f(x) = -u_{\mathrm{ac0}} f(x)$$

For this problem, $p_{\mathrm{ac0}} = 1000$ Pa and $u_{\mathrm{ac0}} = 2.44$ m/s.

Figures 8 and 9 show a series of vorticity and pressure contour plots comparing the new boundary condition VFCBC with the two NSCBC approaches (reflecting and nonreflecting). The scales are the same as in Figs. 2 and 3. In Fig. 9, positive pressure variation contours are represented with dashed lines to visualize the wave front. As expected, the acoustic wave is reflected by the inlet in the case of the reflecting NSCBC method (Fig. 9a), whereas there is no reflection in the case of the two nonreflecting NSCBC and VFCBC methods (Figs. 9b and 9c). The NSCBC nonreflecting method (method 2) is again disqualified by this test case. In Figs. 8b and 9b, the vortex contours are strongly disturbed by the inlet and the

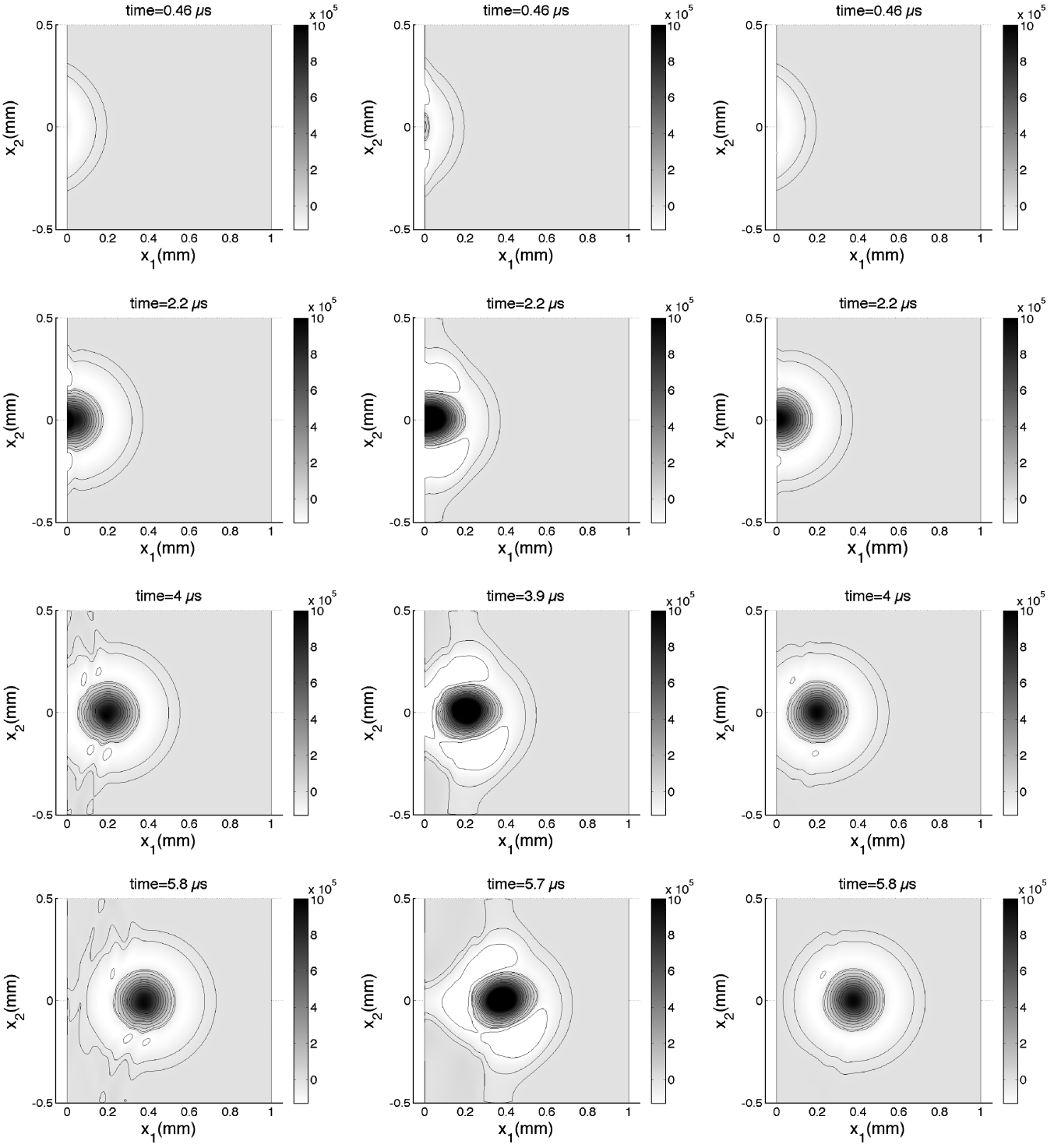

a) NSCBC (Reflecting) **b) NSCBC (Non-reflecting)** **c) VFCBC**

Fig. 8 Vorticity contours $\omega(s^{-1})$.

acoustic wave. The NSCBC reflecting condition (method 1) solution is also affected by the presence of the acoustic wave: after the passage of the acoustic perturbation, deformations appear on the vorticity contours (Fig. 8a). The VFCBC method (method 3) seems to be less sensitive to the perturbation. The solution is only disturbed for a short moment when the vortex and the wave interact.

B. Interaction Between Spatially Decaying Turbulence and a Harmonic Acoustic Wave

To investigate turbulence injection in the presence of acoustics, the outlet pressure is pulsated and harmonic acoustic waves propagate from the reflecting outlet to the inlet in which turbulence is injected. The parameters of the injected turbulence and the computational domain are the same as for the second test case (Fig. 10). The acoustic excitation induces a pressure perturbation p_{ac} on the outlet $x_1 = L$:

$$p_{ac}(L, x_2, t) = p_{ac0} \sin(2\pi f_0 t) \tag{25}$$

where f_0 is the frequency of the acoustic wave. For this problem, $f_0 = 259500$ Hz and $p_{ac0} = 1000$ Pa. The value of f_0 corresponds to the three-quarter-wave mode of the computational box.

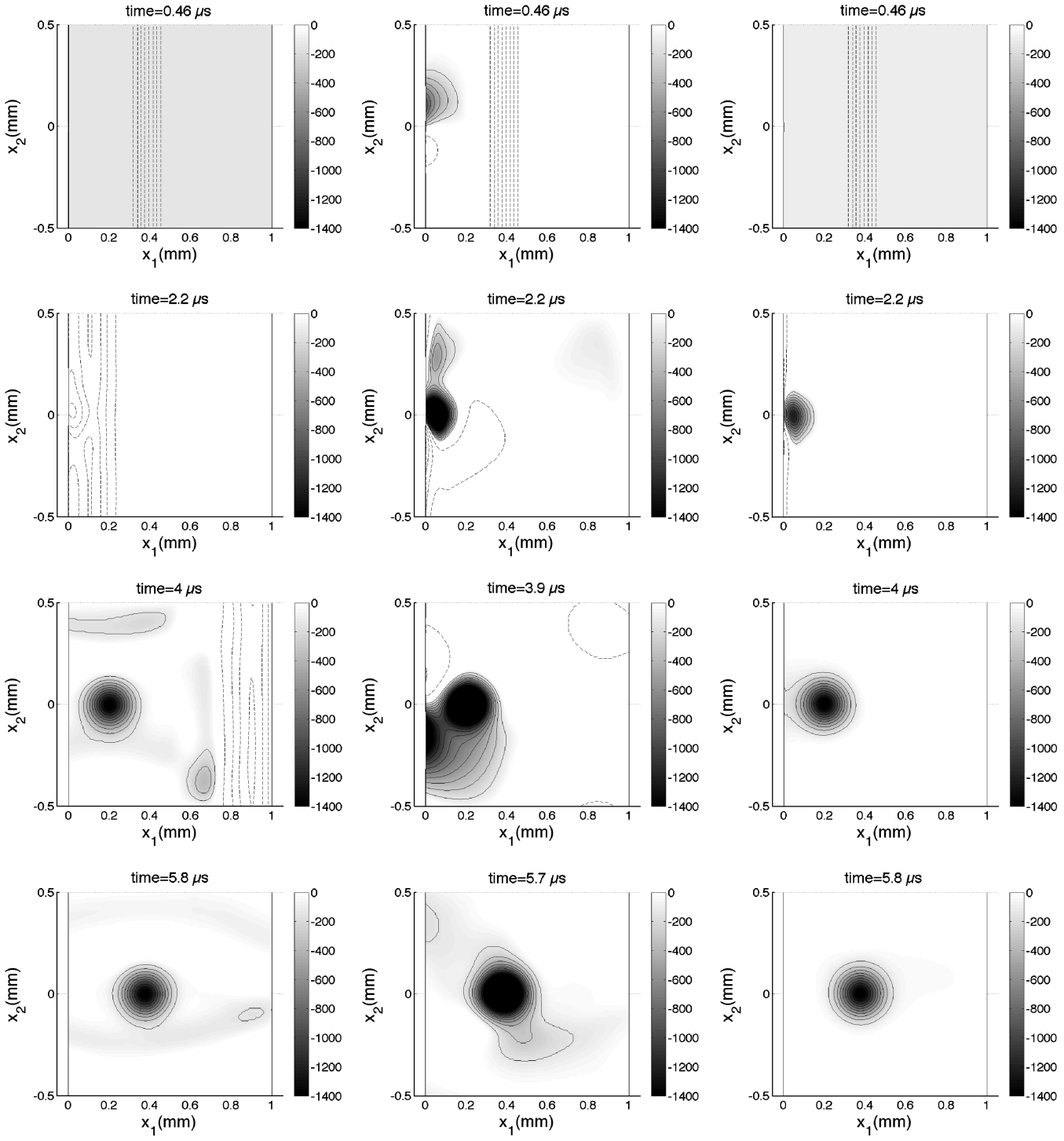

a) NSCBC (Reflecting) **b) NSCBC (Non-reflecting)** **c) VFCBC**

Fig. 9 Pressure contours $P - P_0$ in pascals.

$$f_0 = \frac{3c_0}{4L} \tag{26}$$

This frequency is chosen to mimic cases in which turbulence may have to be injected in a resonant flow.

Using a reflecting or a nonreflecting inlet has a great importance for this test case. For the nonreflecting NSCBC (method 2) and VFCBC (method 3) simulations, the acoustic wave pulsated at the outlet $x_1 = L$ propagates toward the inlet $x_1 = 0$ and leaves the domain. There is no reflection and no acoustic wave travels back to the outlet. Therefore, the acoustic pressure is given by

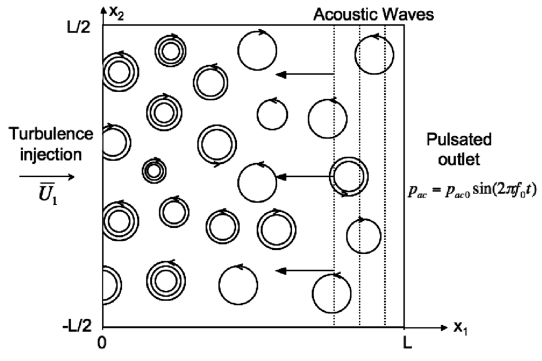

Fig. 10 Sketch of the test case.

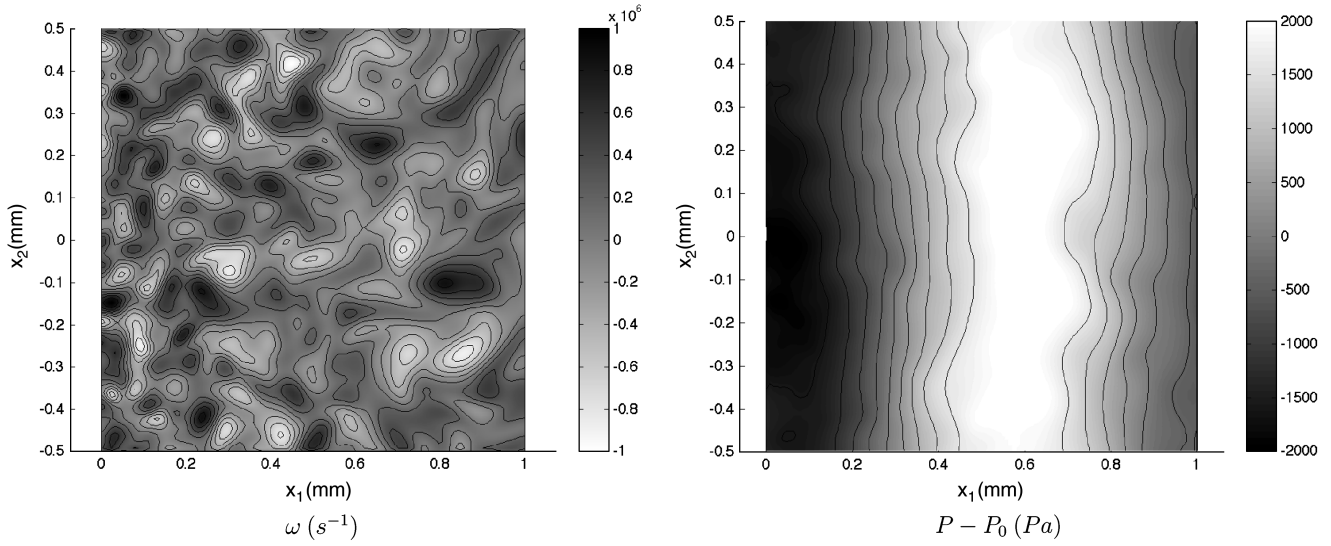

a) NSCBC (Reflecting)

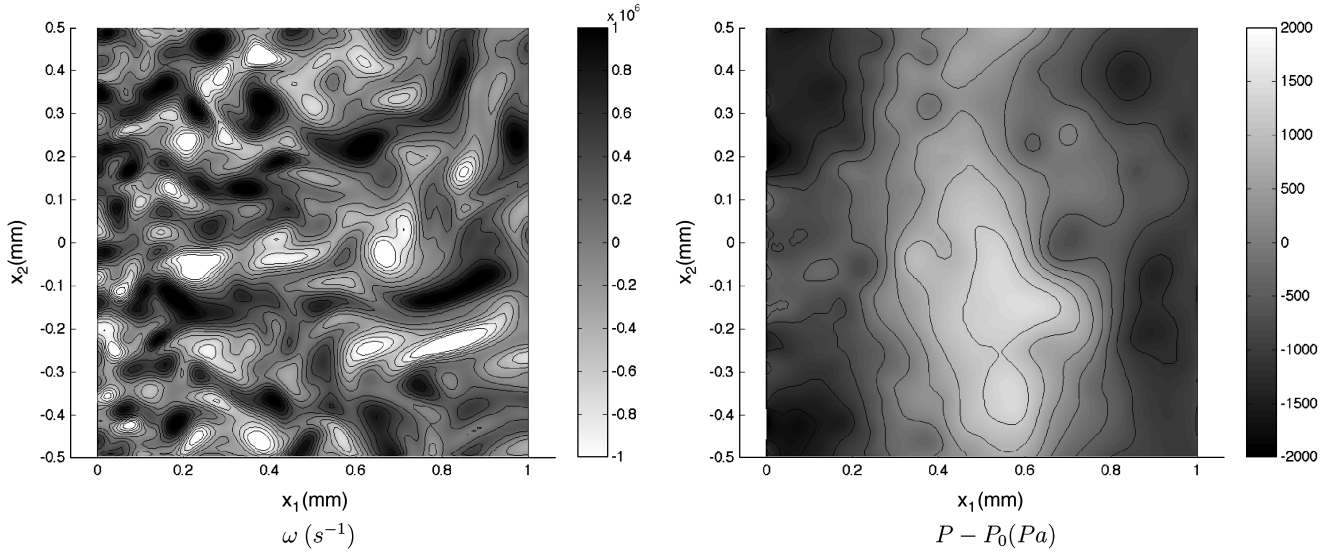

b) NSCBC (Non-reflecting)

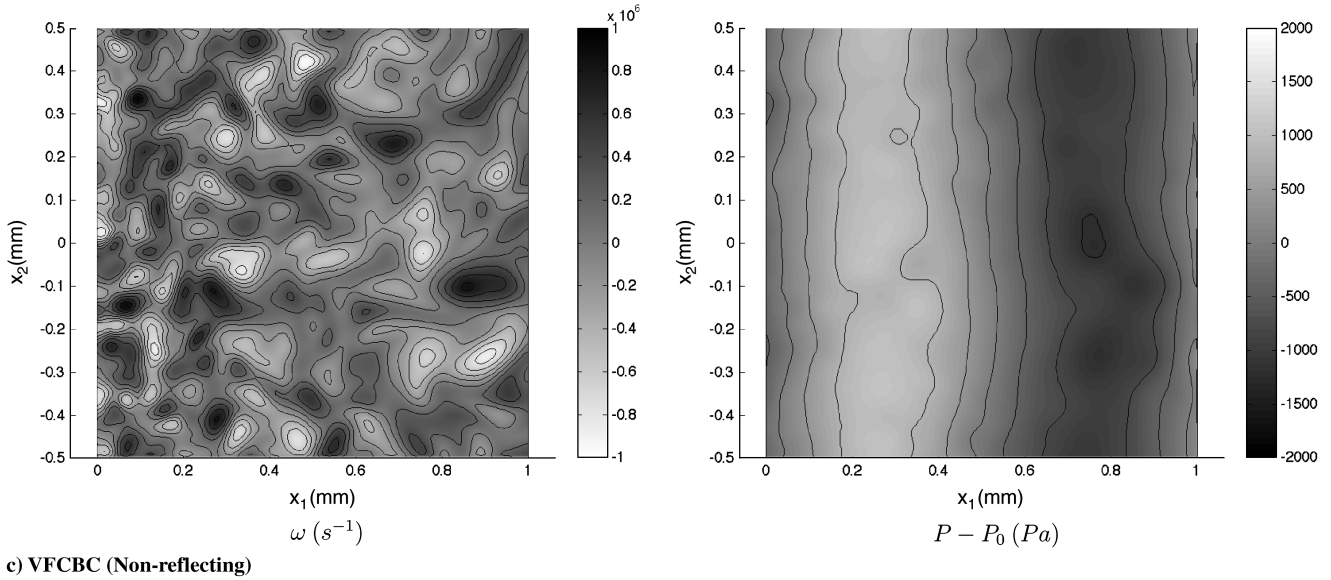

c) VFCBC (Non-reflecting)

Fig. 11 Vorticity and pressure fields of the turbulent flow interacting with a harmonic acoustic wave: $t = 40$ μs.

$$p_{ac}(x_1, x_2, t) = p_{ac0} \sin\left(2\pi f_0 t + \frac{k_0}{1-M}(x_1 - L)\right) \tag{27}$$

where $k_0 = 2\pi f_0/c_0$. The rms acoustic pressure $\sqrt{\overline{p_{ac}^2}}$ is constant and equal to $p_{ac0}/\sqrt{2}$.

In the case of the reflecting NSCBC method (method 1), waves are reflected on the extremities of the box. The superposition of the waves propagating in the two directions generates the development of a stationary longitudinal mode. Spatial and temporal variations may be decoupled by writing

$$p_{ac}(x_1, x_2, t) = \mathcal{R}(p_\omega(x_1) e^{-2\pi i f_0 t}) \tag{28}$$

where $i^2 = -1$, p_ω is a complex number and $\mathcal{R}()$ designates the real part of a complex number. For a low Mach number ($M = u_1/c_0$) and for acoustically closed boundary conditions [$u_{ac}(x_1 = 0) = 0$ and $p_{ac}(x_1 = L) = p_{ac0}\sin(2\pi f_0 t)$], an analytical solution for p_ω exists:

$$p_\omega(x_1) = p_{ac0} \frac{e^{i\beta_+ x_1} + e^{i\beta_- x_1}}{e^{i\beta_+ L} + e^{i\beta_- L}} \tag{29}$$

where $\beta_- = 2\pi f_0/((M-1)c_0)$ and $\beta_+ = 2\pi f_0/((M+1)c_0)$ are the wave numbers for the acoustic waves, respectively, propagating toward the inlet and the outlet. The rms acoustic pressure is not constant, but depends on x_1:

$$\sqrt{\overline{p_{ac}^2}}(x_1) = \sqrt{\frac{p_\omega(x_1) p_\omega^*(x_1)}{2}} \tag{30}$$

where $p_\omega^*(x_1)$ is the conjugate complex of p_ω.

Figure 11 presents instantaneous vorticity and pressure fields for the three methods. Vorticity fields in Figs. 6 and 11 are identical. Contrary to the turbulent flow, the acoustic wave is a 1-D fluctuation and it does not produce any vorticity. Differences between the two test cases actually appear on the pressure fields. In Fig. 11, the acoustic 1-D pressure field p_{ac} is disturbed by pressure contribution due to the turbulent flow. To more quantitatively evaluate the contributions of the two phenomena, pressure profiles at $x_2 = 0$ and $t = 40\ \mu s$ are plotted in Fig. 12. In Fig. 12a, the reflecting NSCBC solution is compared with the stationary longitudinal mode calculated with Eqs. (28) and (29). In Figs. 12b and 12c pressure profiles obtained with the nonreflecting NSCBC and VFCBC methods are compared with the acoustic plane wave propagating toward the inlet [Eq. (27)]. For the reflecting NSCBC method and VFCBC, the contribution of the turbulent flow to the pressure fluctuations is low and the pressure profile is very close to the acoustic pressure. Moreover, turbulence injected with the nonreflecting NSCBC is very noisy and turbulent pressure fluctuations reach the same level as the acoustic pressure.

Figure 13 presents the average properties of the flow versus distance to the injection plane. For the nonreflecting NSCBC and VFCBC methods, the kinetic energy K_0 is not disturbed by the acoustic wave: the acoustic velocity u_{ac0} created by the pulsation is much smaller than the turbulent velocity of the flow and does not modify K_0 significatively. In the case of the reflecting NSCBC simulation, the three-quarter-wave mode locally generates high levels of acoustic velocity fluctuations that modify the field of kinetic energy (Fig. 13a). As expected, the dissipation rate in Fig. 13b is identical to the test case without acoustic pulsation for all three methods, because the pulsating outlet induces a 1-D acoustic wave that does not generate vorticity.

For this test case, the average fluctuating pressure in Fig. 13c is normalized by $p_{ac0}/\sqrt{2}$. Contrary to the velocity, the acoustic perturbation generates much higher pressure fluctuations than the turbulence. Typically, for the VFCBC method, pressure fluctuations remain nearly constant and equal to the theoretical value $p_{ac0}/\sqrt{2}$, corresponding to the solution of the acoustic problem with a nonreflecting inlet. The nonreflecting NSCBC method creates levels of pressure that are too high in comparison with the theory. These discrepancies may be explained by the fact that this boundary condition generates levels of turbulent pressure fluctuations that are not negligible compared with the acoustic pressure fluctuations. The theoretical curve corresponding to the three-quarter-wave mode is shown by a solid line in Fig. 13c. It matches the curve corresponding to the reflecting NSCBC simulation. Differences only occur when the average fluctuating pressure is close to zero and reaches the same order as the turbulent dynamic pressure ρK_0.

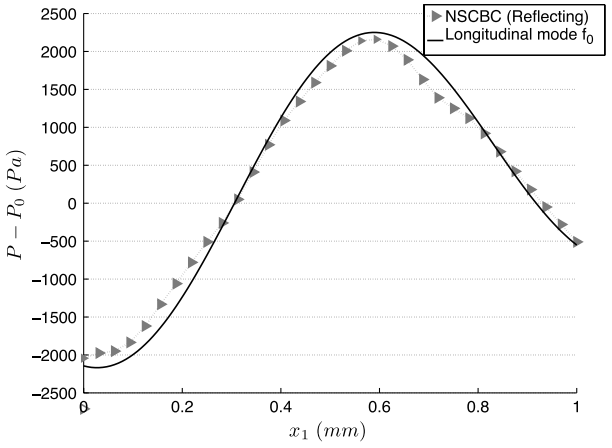

a) NSCBC (Reflecting)

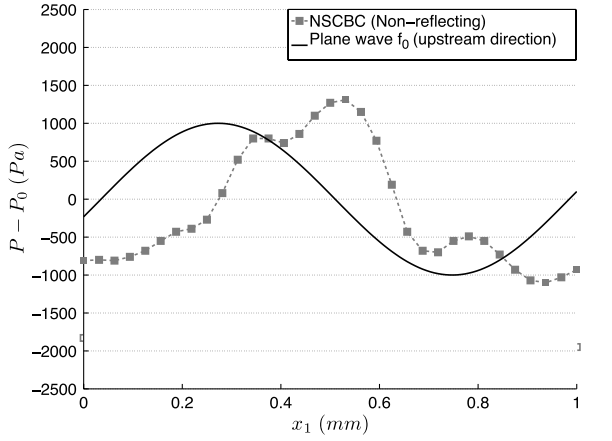

b) NSCBC (Non-reflecting)

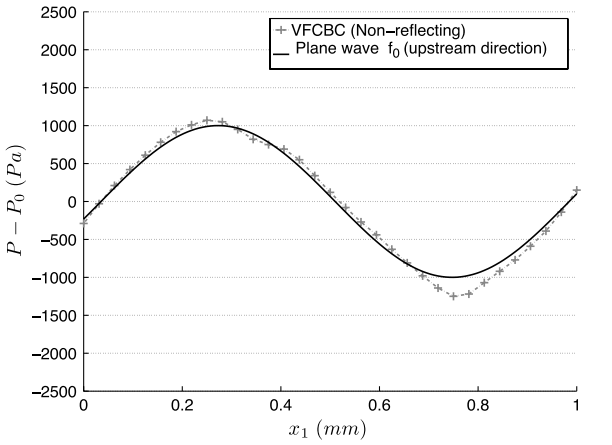

c) VFCBC (Non-reflecting)

Fig. 12 Streamwise evolution of the mean properties of the turbulent flow coupled to the harmonic wave f_0. Comparison of the three boundary conditions.

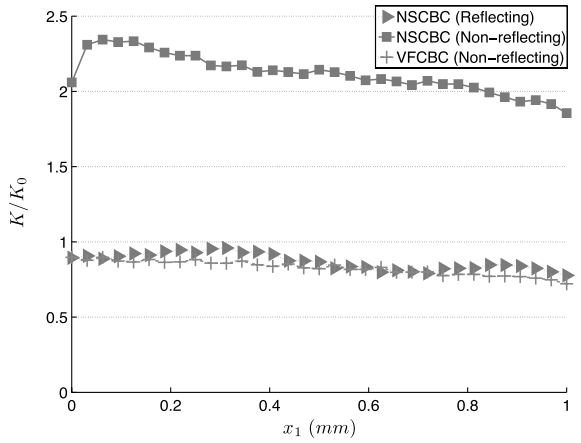

a) Normalized turbulent kinetic energy K/K_0

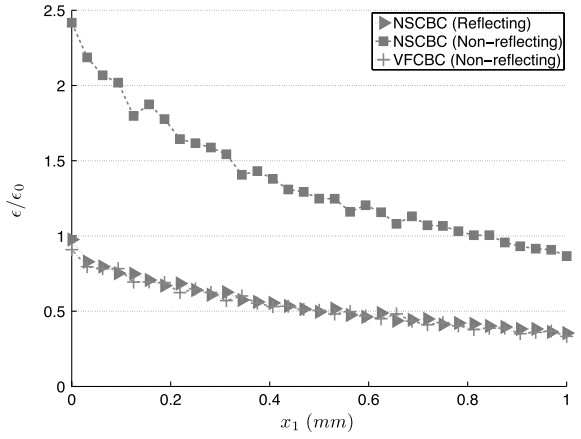

b) Normalized dissipation rate ϵ/ϵ_0

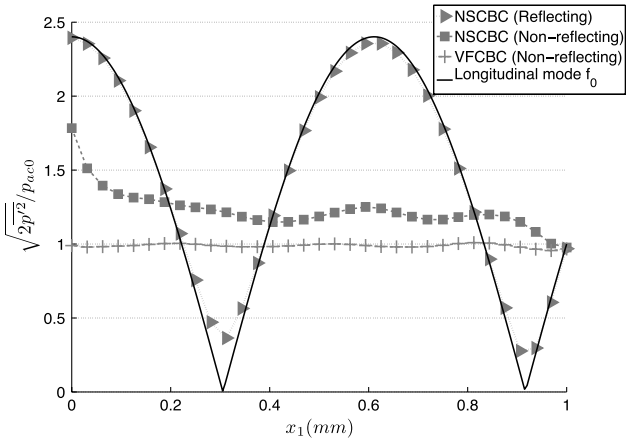

c) Normalized pressure fluctuations

Fig. 13 Streamwise evolution of the mean properties of the turbulent flow coupled to the harmonic wave f_0. Comparison of the three boundary conditions.

VI. Conclusions

Introducing turbulent fluctuations in DNS or LES is required for multiple applications. This task becomes difficult in compressible solvers in which boundary conditions must allow turbulence injection but also control of acoustic waves. This paper compares three boundary conditions for compressible solvers to inject vortices or turbulence through an inlet while controlling reflections (all methods use characteristic approaches):

1) Method 1 is a fully reflecting method based on the NSCBC technique.

2) Method 2 is a fully nonreflecting method based on the NSCBC technique; this method is the classical perfectly nonreflecting approach for acoustic waves.

3) Method 3 is a new nonreflecting method called VFCBC (vortical-flow characteristic boundary conditions) which was developed for this work.

The three methods are systematically compared on two cases of growing complexity: 1) a two-dimensional vortex entering a quiet domain and 2) a two-dimensional synthetic turbulent flow entering a quiet domain.

Tests are then repeated by adding an acoustic wave interacting with the inlet for the 2-D vortex and a harmonic wave injected by the outlet for the turbulent case. Results show that method 2, which is well suited to let acoustic waves propagate through an inlet without reflections, is not adapted to introducing vortices or turbulence: the vorticity field is distorted during the vorticity wave introduction. Method 1 allows introducing vortices or turbulence, but totally reflects any acoustic wave hitting the outlet at the same time. Method 3 performs as well as method 1 for vorticity waves, but allows outgoing waves to leave the domain without reflections. Methods 1 and 3 are simple to implement and should be useful for LES and DNS of compressible flows such as jet noise, cavity noise, combustion instabilities in combustion chambers, etc.

Acknowledgments

We thank Laurent Selle (Institut de Mécanique des Fluides de Toulouse, Centre National de la Recherche Scientifique) for helpful discussions and the Centre Européen de Recherche et de Formation Avancée en Calcul Scientifique computational fluid dynamics (CFD) team staff for their scientific and technical support about the CFD code AVBP. The first author gratefully acknowledges the funding by Air Liquide and the support of Centre Informatique National de l'Enseignement Supérieur for computing time.

References

[1] Thompson, K. W., "Time Dependent Boundary Conditions for Hyperbolic Systems," *Journal of Computational Physics*, Vol. 89, No. 2, 1990, pp. 439–461. doi:10.1016/0021-9991(90)90152-Q

[2] Grappin, R., Léorat, J., and Buttighoffer, A., "Alfvén Wave Propagation in the High Solar Corona," *Astronomy and Astrophysics*, Vol. 362, 2000, pp. 342–358.

[3] Freund, J. B., "Proposed Inflow/Outflow Boundary Condition for Direct Computation of Aerodynamic Sound," *AIAA Journal*, Vol. 35, No. 4, 1997, pp. 740–742. doi:10.2514/2.167

[4] Colonius, T., "Numerically Nonreflecting Boundary and Interface Conditions for Compressible Flow and Aeroacoustic Computations," *AIAA Journal*, Vol. 35, No. 7, 1997, pp. 1126–1133. doi:10.2514/2.235

[5] Colonius, T., and Lele, S. K., "Computational Aeroacoustics: Progress on Nonlinear Problems of Sound Generation," *Progress in Aerospace Sciences*, Vol. 40, No. 6, 2004, pp. 345–416. doi:10.1016/j.paerosci.2004.09.001

[6] Bogey, C., and Bailly, C., "Effects of Inflow Conditions and Forcing on Subsonic Jet Flows and Noise," *AIAA Journal*, Vol. 43, No. 5, 2005, pp. 1000–1007. doi:10.2514/1.7465

[7] Poinsot, T., and Veynante, D., *Theoretical and Numerical Combustion*, 2nd ed., R. T. Edwards, Philadelphia, 2005.

[8] Schmitt, P., Poinsot, T. J., Schuermans, B., and Geigle, K., "Large-Eddy Simulation and Experimental Study of Heat Transfer, Nitric Oxide Emissions and Combustion Instability in a Swirled Turbulent High Pressure Burner," *Journal of Fluid Mechanics*, Vol. 570, 2007, pp. 17–46. doi:10.1017/S0022112006003156

[9] Poinsot, T., and Lele, S., "Boundary Conditions for Direct Simulations of Compressible Viscous Flows," *Journal of Computational Physics*, Vol. 101, No. 1, 1992, pp. 104–129. doi:10.1016/0021-9991(92)90046-2

[10] Thompson, K. W., "Time Dependent Boundary Conditions for Hyperbolic Systems," *Journal of Computational Physics*, Vol. 68, No. 1, 1987, pp. 1–24.

doi:10.1016/0021-9991(87)90041-6
[11] Giles, M., "Nonreacting Boundary Conditions for Euler Equation Calculations," *AIAA Journal*, Vol. 28, No. 12, 1990, pp. 2050–2058. doi:10.2514/3.10521
[12] Moureau, V., Lartigue, G., Sommerer, Y., Angelberger, C., Colin, O., and Poinsot, T., "High-Order Methods for DNS and LES of Compressible Multi-Component Reacting Flows on Fixed and Moving Grids," *Journal of Computational Physics*, Vol. 202, No. 2, 2005, pp. 710–736. doi:10.1016/j.jcp.2004.08.003
[13] Poinsot, T., Veynante, D., and Candel, S., "Quenching Processes and Premixed Turbulent Combustion Diagrams," *Journal of Fluid Mechanics*, Vol. 228, 1991, pp. 561–605. doi:10.1017/S0022112091002823
[14] Baum, M., Poinsot, T., Haworth, D., and Darabiha, N., "Using Direct Numerical Simulations to Study $H_2/O_2/N_2$ Flames with Complex Chemistry in Turbulent Flows," *Journal of Fluid Mechanics*, Vol. 281, 1994, pp. 1–32. doi:10.1017/S0022112094003010
[15] Jiménez, C., Cuenot, B., Poinsot, T., and Haworth, D., "Numerical Simulation and Modeling for Lean Stratified Propane-Air Flames," *Combustion and Flame*, Vol. 128, Nos. 1–2, 2002, pp. 1–21. doi:10.1016/S0010-2180(01)00328-5
[16] Lignell, D. O., Chen, J. H., Smith, P. J., Lu, T., and Law, C. K., "The Effect of Flame Structure on Soot Formation and Transport in Turbulent Nonpremixed Flames Using Direct Numerical Simulation," *Combustion and Flame*, Vol. 151, Nos. 1–2, 2007, pp. 2–28. doi:10.1016/j.combustflame.2007.05.013
[17] Selle, L., Lartigue, G., Poinsot, T., Koch, R., Schildmacher, K.-U., Krebs, W., Prade, B., Kaufmann, P., and Veynante, D., "Compressible Large-Eddy Simulation of Turbulent Combustion in Complex Geometry on Unstructured Meshes," *Combustion and Flame*, Vol. 137, No. 4, 2004, pp. 489–505. doi:10.1016/j.combustflame.2004.03.008
[18] Roux, S., Lartigue, G., Poinsot, T., Meier, U., and Bérat, C., "Studies of Mean and Unsteady Flow in a Swirled Combustor Using Experiments, Acoustic Analysis and Large Eddy Simulations," *Combustion and Flame*, Vol. 141, Nos. 1–2, 2005, pp. 40–54. doi:10.1016/j.combustflame.2004.12.007
[19] Sengissen, A., Giauque, A., Staffelbach, G., Porta, M., Krebs, W., Kaufmann, P., and Poinsot, T., "Large Eddy Simulation of Piloting Effects on Turbulent Swirling Flames," *Proceedings of the Combustion Institute*, Vol. 31, No. 2, 2007, pp. 1729–1736. doi:10.1016/j.proci.2006.07.010
[20] Yoo, C., Wang, Y., Trouvé, A., and Im, H., "Characteristic Boundary Conditions for Direct Simulations of Turbulent Counterow Flames," *Combustion Theory and Modeling*, Vol. 9, No. 4, 2005, pp. 617–646. doi:10.1080/13647830500307378
[21] Yoo, C., and Im, H., "Characteristic Boundary Conditions for Simulations of Compressible Reacting Flows with Multidimensional, Viscous, and Reaction Effects," *Combustion Theory and Modeling*, Vol. 11, No. 2, 2007, pp. 259–286. doi:10.1080/13647830600898995
[22] Lodato, G., Domingo, P., and Vervisch, L., "Three-Dimensional Boundary Conditions for Direct and Large-Eddy Simulation of Compressible Viscous Flow," *Journal of Computational Physics*, Vol. 227, No. 10, 2008, pp. 5105–5143. doi:10.1016/j.jcp.2008.01.038
[23] Prosser, R., "Improved Boundary Conditions for the Direct Numerical Simulation of Turbulent Subsonic Flows 1: Inviscid Flows," *Journal of Computational Physics*, Vol. 207, No. 2, 2005, pp. 736–768. doi:10.1016/j.jcp.2005.01.027
[24] Prosser, R., "Towards Improved Boundary Conditions for the DNS and LES of Turbulent Subsonic Flows," *Journal of Computational Physics*, Vol. 222, No. 2, 2007, pp. 469–474. doi:10.1016/j.jcp.2006.09.006
[25] Bogey, C., and Bailly, C., "Computation of a High Reynolds Number Jet and Its Radiated Noise Using Large Eddy Simulation Based on Explicit Filtering," *Computers and Fluids*, Vol. 35, No. 10, 2006, pp. 1344–1358. doi:10.1016/j.compfluid.2005.04.008
[26] Prière, C., Gicquel, L. Y. M., Gajan, P., Strzelecki, A., Poinsot, T., and Bérat, C., "Experimental and Numerical Studies of Dilution Systems for Low Emission Combustors," *AIAA Journal*, Vol. 43, No. 8, 2005, pp. 1753–1766. doi:10.2514/1.14681
[27] Guichard, L., Réveillon, J., and Hauguel, R., "Direct Numerical Simulation of Statistically Stationary One- and Two-Phase Turbulent Combustion: A Turbulent Injection Procedure," *Flow, Turbulence and Combustion*, Vol. 73, No. 2, 2004, pp. 133–167. doi:10.1023/B:APPL.0000049273.27776.f5
[28] Domingo, P., Vervisch, L., and Réveillon, J., "DNS Analysis of Partially Premixed Combustion in Spray and Gaseous Turbulent Flame-Bases Stabilized in Hot Air," *Combustion and Flame*, Vol. 140, No. 3, 2005, pp. 172–195. doi:10.1016/j.combustflame.2004.11.006
[29] Klein, M., Sadiki, A., and Janicka, J., "Investigation of the Influence of the Reynolds Number on a Plane Jet Using Direct Numerical Simulation," *International Journal of Heat and Fluid Flow*, Vol. 24, No. 6, 2003, pp. 785–794. doi:10.1016/S0142-727X(03)00089-4
[30] Klein, M., Sadiki, A., and Janicka, J., "A Digital Filter Based Generation of Inflow Data For Spatially Developing Direct Numerical or Large Eddy Simulations," *Journal of Computational Physics*, Vol. 186, No. 2, 2003, pp. 652–665. doi:10.1016/S0021-9991(03)00090-1
[31] Smirnov, A., Shi, S., and Celik, I., "Random Flow Generation Technique for Large Eddy Simulations and Particle-Dynamics Modeling," *Journal of Fluids Engineering*, Vol. 123, No. 2, 2001, pp. 359–371. doi:10.1115/1.1369598
[32] Lee, S., Lele, S., and Moin, P., "Simulation of Spatially Evolving Turbulence and the Applicability of Taylor's Hypothesis in Compressible Flows," *Physics of Fluids A*, Vol. 4, No. 7, 1992, pp. 1521–1530. doi:10.1063/1.858425
[33] Poinsot, T., Echekki, T., and Mungal, M. G., "A Study of the Laminar Flame Tip and Implications for Premixed Turbulent Combustion," *Combustion Science and Technology*, Vol. 81, Nos. 1–3, 1992, pp. 45–73. doi:10.1080/00102209208951793
[34] Kaufmann, A., Nicoud, F., and Poinsot, T., "Flow Forcing Techniques for Numerical Simulation of Combustion Instabilities," *Combustion and Flame*, Vol. 131, No. 4, 2002, pp. 371–385. doi:10.1016/S0010-2180(02)00419-4
[35] Yoo, C. S., and Im, H. G., "Characteristic Boundary Conditions for Simulations of Compressible Reacting Flows with Multi-Dimensional, Viscous, and Reaction Effects," *Combustion Theory and Modeling*, Vol. 11, No. 2, 2007, 259–286. doi:10.1080/13647830600898995
[36] Colonius, T., Lele, S., and Moin, P., "The Free Compressible Vortex," *Journal of Fluid Mechanics*, Vol. 230, 1991, pp. 45–73. doi:10.1017/S0022112091000708
[37] Colin, O., and Rudgyard, M., "Development of High-Order Taylor-Galerkin Schemes for Unsteady Calculations," *Journal of Computational Physics*, Vol. 162, No. 2, 2000, pp. 338–371. doi:10.1006/jcph.2000.6538
[38] Celik, I., Yavuz, I., and Smirnov, A., "Large Eddy Simulations of In-Cylinder Turbulence for Internal Combustion Engines: A Review," *International Journal of Engine Research*, Vol. 2, No. 2, 2001, pp. 119–148. doi:10.1243/1468087011545389
[39] Kraichnan, R., "Diffusion by a Random Velocity Field," *Physics of Fluids*, Vol. 13, 1970, pp. 22–31. doi:10.1063/1.1692799

C. Bailly
Associate Editor